APPLICATION OF A BODY FORCE APPROACH FOR NUMERICAL HEAT EXCHANGER SIMULATIONS WITHIN A HYBRID ELECTRIC PROPULSION AIRCRAFT CONCEPT

J. Kirz, A.-R. Hübner, S. Spinner
German Aerospace Center (DLR), Institute of Aerodynamics and Flow Technology,
Lilienthalplatz 7, 38108 Braunschweig, Germany

K. Weinman
German Aerospace Center (DLR), Institute of Aerodynamics and Flow Technology,
Bunsenstraße 10, 37073 Göttingen, Germany

Abstract

Hybrid electric propulsion concepts have a great potential to reduce the overall emissions of aviation. For fuel cell applications heat exchangers are required to dissipate the waste heat produced by the fuel cell. The integration of the heat exchangers has an impact on the aircraft aerodynamics which in turn is influencing the flow through the cooler duct. This paper presents a new approach in the DLR TAU Code to model a heat exchanger using the body force method in the Flowsimulator framework. The results are verified using analytic solutions and OpenFoam simulations. The results indicate that the approach is robust and properly resolving the underlying physics. The comparison between the analytic solution and the new heat exchanger model is very good. Fine grid resolutions are necessary to resolve the flow through the cooler properly. First applications for the new method are shown for a fuselage-mounted cooler as well as for a nacelle-mounted cooler.

1. INTRODUCTION AND OBJECTIVE

The European Green Deal targets a reduction of net greenhouse gas emissions by at least 55% by 2030 when compared to 1990 levels. Current studies suggest that aviation is responsible for about 3.3% of the total CO_2 emissions [1]. In order to achieve the goals of the green deal and reduce CO_2 emissions for aircraft new propulsion concepts are proposed which include hydrogen and electric flight.

In 2020, DLR published the white paper 'Zero Emission Aviation' together with the German Aerospace Industries Association (BDLI) [2] and is currently working on a Zero Emission strategy. The European Commission launched a new Alliance for Zero Emission Aviation during 2020 as an initiative to prepare Europe for hydrogen and electric flight.

First research flight demonstrators of novel aircraft concepts are being developed and built, for example the NASA X-57 Maxwell or the DLR/MTU Dornier 228 Electric Flight Demonstrator.

Some of the novel aircraft concepts utilize hybrid electric propulsion (HEP) whereby electric motors are used to generate thrust and a fuel cell is installed to generate the electrical power for the motors. Studies show that aircraft powered by a hydrogen fuel cell have the potential to reduce the total climate impact by 75-90% when compared to kerosene-powered aircraft [3].

While the overall energy efficiency of hydrogen hybrid electric aircraft is superior to conventional aircraft, current fuel cells achieve efficiency levels of about 40-60% depending on the fuel cell type [4]. Consequently, a significant share of the energy stored in the fuel is converted into waste heat. Thus, a heat exchanger integrated into a fairing cooler is required for heat dissipation. This presents an additional requirement for aircraft design and certification. The assembly consisting of a heat exchanger and a fairing is referred to as cooler in this paper.

While many studies currently performed focus on propulsion integration, tank integration, heat exchanger optimization or ground infrastructure for hybrid electric aircraft, the integration of the cooler is often not considered in detail. However, DLR has identified the aerodynamic integration of the heat exchanger as a critical aspect in the clean sheet or retro-fit design of hybrid electric aircraft. In order to dissipate enough heat, the size of the cooler can be significant.
On one hand the heat exchanger performance is influenced by aircraft aerodynamics. The largest cooling requirement is needed at take-off and climb when the velocity of the aircraft is very low and the angle of attack is very high, both negatively impacting the achievable heat exchanger effectiveness. On the other hand, the aerodynamics of the aircraft are influenced by the heat exchanger, e.g. due to a significant drag penalty. Thus, an appropriate aerodynamic cooler integration is key for this aircraft concept to achieve stable and safe flight.

In consequence, it becomes more and more important to numerically simulate and analyze heat exchanger designs integrated into complex aircraft geometries. Established CFD codes must provide physically accurate and robust methods in order to assess the impact of the heat exchanger on the overall aircraft aerodynamics.

This paper presents an extension of the body force method implemented in the Flowsimulator Framework of the DLR TAU Code to simulate heat exchangers with a focus on the influence of heat exchanger operation on overall aircraft performance.

2. IMPLEMENTATION

Previously the DLR TAU Code offered two methods capable of modelling a heat exchanger: The *Heat Exchanger* 1D boundary condition [5] and the *Actuator Disk* approach [6]. However, the methods are complicated to apply for the simulation of heat exchangers or were not robust for the challenging flow conditions. Thus, in this work an existing state of the art engine modeling method for the DLR TAU code [7] is modified and applied to the simulation of heat exchangers. It is based on body force modeling using the Flowsimulator framework.

The Flowsimulator framework is coupled to the DLR TAU Code via a Python interface. The body force modeling utilizes this interface and is mainly applied today to simulate conventional turbofan engines. Studies have shown that mean turbomachinery aerodynamics are accurately resolved for different flow conditions and operating points [7]. Therefore, it was assumed that the body forces approach would also be suitable to simulate heat exchangers. Due to its capability to resolve three-dimensional effects, it has the potential to be superior to 1D boundary conditions or actuator disk approaches. The approach taken is similar to that adopted in other CFD codes, such as CFX, as well as OpenFOAM.

Experimental data for on-board cooler systems (under flight conditions) is not readily available and the problem at one on-flow velocity condition was analyzed using the open-source OpenFOAM package [8]. This calculation provides an additional cross-check on the implementation of the body force method within the Flowsimulator package. Internal flow analysis (including heat exchanger performance estimates) are well validated in OpenFOAM in both academic and industrial applications. Standard OpenFOAM Function objects were used to add source terms to the momentum and energy equations:

The body force interface was extended according to the physics of a heat exchanger (HEX). The implementation is based on a filtering of the grid to identify the cells where HEX source terms are active. The HEX is characterized by a pressure drop Δp and a heat flux q̇. Three different ways to account for this pressure drop and heat flux are implemented:

1) Constant values of Δp and q̇ are specified by the user.
2) q̇ is specified by the user and Δp is calculated from Forchheimer's equation by specifying the permeability coefficients K and k_2 [9]:

   (1) $-\frac{dp}{dx} = \frac{\eta}{K}u + \frac{\rho}{k_2}u^2$.

3) The Flowsimulator Python framework is coupled to a lookup table based on a 1D-model of the heat exchanger. Δp and q̇ are iteratively converged within the CFD simulation based on flow states through the cooler.

In order to verify the correct numerical implementation of the body force model and the details of its application for heat exchangers, the focus of this paper is option 1 where the pressure drop and heat flux are specified by the user. A source term $\vec{f}$ for the pressure drop is added to the momentum equations while a source term f_Θ for the heat flux is added to the energy equation within the filtered volume. More details about the source terms specified for the body force method are provided in Ref [10].

In this version of the body force heat exchanger (BFHEX) the complex flow through the HEX is simplified by assuming a uniform distribution of the induced momentum and energy within the filtered volume.

3. TEST CASE SETUP

A generic geometry is used as a test case for the cooler setup. FIG 1 shows the test case geometry. An isolated and axisymmetric nacelle with a length of 2m and an inner radius of 0.4m was modelled. The HEX region is 0.5m long and starts 0.75m behind the inlet lip of the nacelle. The resulting cross-sectional area of the HEX is 0.5m² and the resulting volume is 0.25m³.

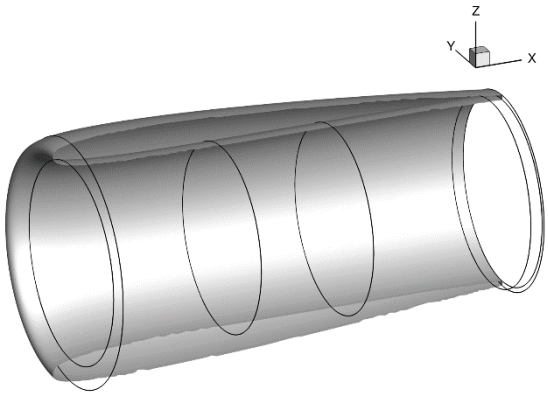

FIG 1. Generic nacelle test case geometry for the heat exchanger simulation verification.

3.1. Grid Generation

The commercial grid generation software CENTAUR was used to generate hybrid grids of the axisymmetric nacelle. The boundary layer is resolved with prisms while tetrahedra are used for the remaining volume. In order to assess the impact of the grid resolution on the results, grids at three different refinement levels were generated. Refinement sources were used within the cooler duct to specify the cell edge length. An overview of the generated grids is provided in TAB 1.

Grid resolution	Cells per HEX length	Cell edge length	Number of nodes
Coarse	10	50 mm	2.94 mio.
Medium	20	25 mm	3.08 mio.
Fine	40	12.5 mm	4.22 mio.
OpenFoam	120	3.125 mm	120 mio

TAB 1. Overview of the grids.

Based on these grids, three derivatives were generated where the HEX volume was resolved using a structed grid block consisting of hexahedra. This setup is shown for the finest grid resolution in FIG 2.

For the OpenFOAM method the cooler surface was extracted from the medium CENTAUR mesh and OpenFOAM methods were then used to generate a volume mesh. The volume mesh is significantly finer than the fine TAU mesh as the function of the OpenFOAM calculation

was to provide a reference solution. It should also be noted that OpenFOAM can be considered as based on an extended Cartesian approach for which accurate computation on highly stretched boundary layer cells could be problematic.

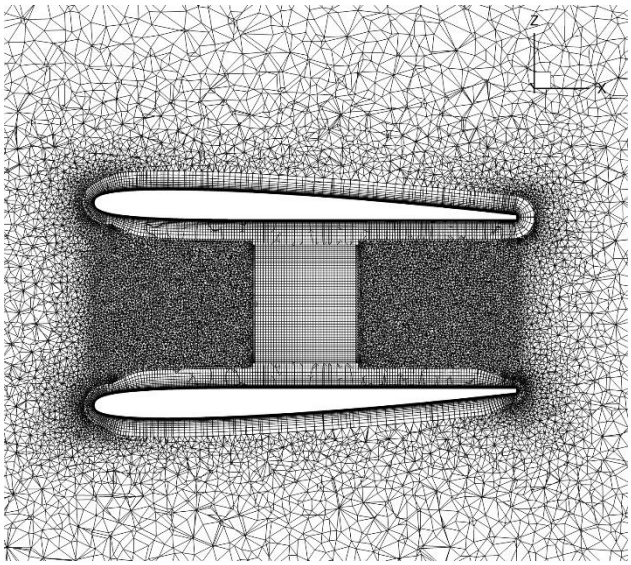

FIG 2. CENTAUR grid with hexahedral cells in the HEX block (fine grid resolution with 12.5mm cell edge length in the cooler duct).

3.2. Numerical Setup

The DLR TAU code [11] is a vertex-based CFD solver based on an unstructured finite-volume approach for solving the Euler or Reynolds-averaged Navier-Stokes (RANS) equations on hybrid grids. It was primarily developed for external aerodynamic applications. All TAU simulations presented in this paper were performed fully turbulent using the Spalart Allmaras one-equation turbulence model [12]. A second order central differencing scheme with matrix dissipation is applied for the spatial discretization of the convective fluxes and an implicit lower upper symmetric Gauss Seidel scheme is used for time stepping.

Parameter	Value
Reference pressure (p_∞)	101325 Pa
Reference temperature (T_∞)	288.15 K
Reference velocity (u_∞)	50 m/s
Heat flux ($\dot{q}$)	100 kW
Pressure drop (Δp)	1000 Pa

TAB 2. Reference settings for the simulation and setup of the heat exchanger.

The reference conditions used for the simulation as well as the specified HEX parameters are summarized in TAB 2. FIG 3 illustrates a cut through the symmetry plane of the test case geometry and provides an overview of the volume within which the body forces are active.

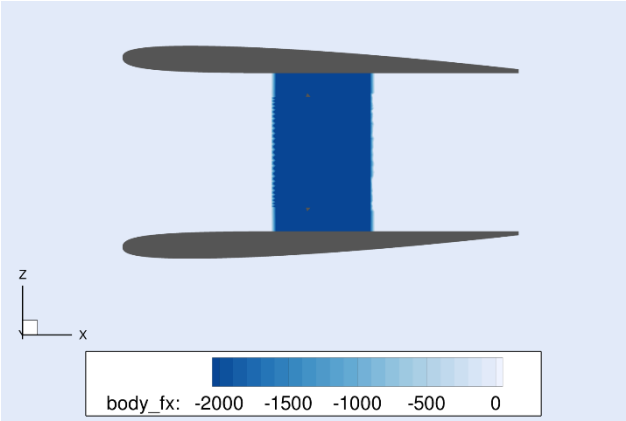

FIG 3. Visualization of the filtered numerical domain (body force volume).

4. TEST CASE RESULTS

The focus of this paper is the verification of the implementation of the heat exchanger. Additionally, the impact of the grid resolution on the results is presented.

4.1. Verification of the Implementation

In order to verify the implementation of the new heat exchanger simulation method, four simulations were performed with different HEX settings and the results are discussed in this section. A list of the simulations undertaken with HEX operating parameters is provided in TAB 3. The objective of this study is to verify the impact of the pressure drop and the heat flux on the flow within the cooler. Thus, two simulations with either only the pressure drop or only the heat flux activated were performed. These simulations do not represent physical flow states but are very valuable for the verification. In addition to these simulations a heat exchanger simulation with both the pressure drop and the heat flux activated, as well as a through-flow nacelle without BFHEX are simulated as references. gives an overview of the simulations and the BFHEX setting used.

Setting	Heat flux $\dot{q}$	Pressure drop Δp
Δp and $\dot{q}$	100 kW	10 hPa
Δp only	0 kW	10 hPa
$\dot{q}$ only	100 kW	0 hPa
flow through	0 kW	0 hPa

TAB 3. Overview of simulations performed for the verification of the BFHEX method

FIG 4 provides an overview of the results by showing lines extracted from the field solutions along the axis of rotation of the cooler. The light grey area highlights the nacelle. The extent of the heat exchanger is marked by the dark grey area. The simulation with the heat exchanger activated shows a significantly reduced velocity within the nacelle compared to the through-flow nacelle. This is mainly a consequence of the pressure gradient due to the heat exchanger. The impact of the heat flux on the static pressure and velocity is small compared to the impact of the pressure gradient on these variables.

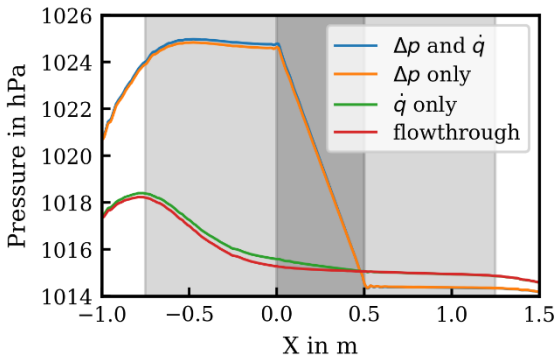

a) Static pressure

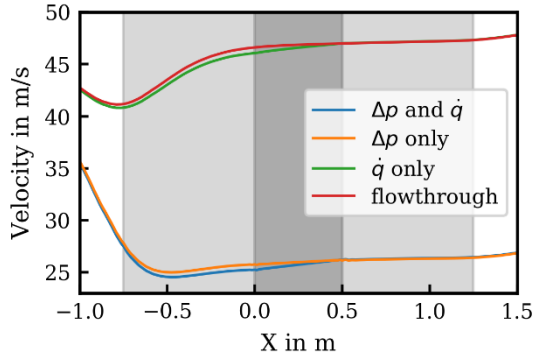

b) Velocity

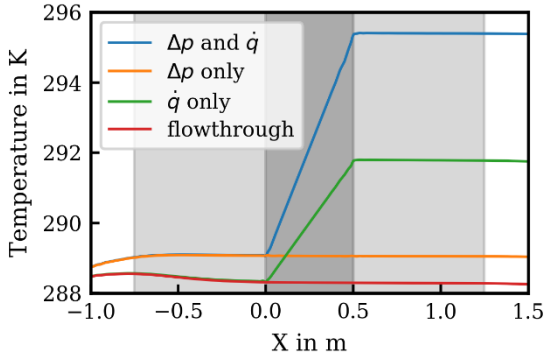

c) Static temperature

FIG 4. Pressure, velocity, and temperature along the centerline of the nacelle for different numerical settings.

The pressure drop can directly be verified in FIG 4a) and corresponds well to the prescribed pressure drop. The verification of the heat flux is slightly more complicated. The temperature rise of a fluid with specified heat input and mass flow can be estimated according to the following equation:

(2) $\Delta T = T_2 - T_1 = \frac{\dot{q}}{\dot{m} \cdot c_p}$.

Here $\dot{m}$ is the mass flow rate and c_p is the specific heat capacity of air calculated approximately as follows:

(3) $c_p = \frac{\kappa R}{\kappa - 1} \approx 1000 \frac{J}{kg \cdot K}$.

The mass flow can be calculated from the velocity u, the density ρ and the cross-sectional area A of the nacelle:

(4) $\dot{m} = \rho \cdot u \cdot A$.

Using the velocities shown in FIG 4b) as input this leads to the following results for a density of 1.22kg/m³ and a heat flux of 100kW:

- $\dot{m}\left(u = 25.5 \frac{m}{s}\right) \approx 15.6 \frac{kg}{s} \rightarrow \Delta T \approx 6.4K$
- $\dot{m}\left(u = 46.2 \frac{m}{s}\right) \approx 28.6 \frac{kg}{s} \rightarrow \Delta T \approx 3.5K$.

These estimations for the temperature increase within the heat exchanger correspond very well to the results of the simulation shown in FIG 4c). Additionally, the TAU and OpenFoam results compare very well with an active heat exchanger as shown in FIG 5. The offset in pressure and velocity for the flow-through simulations results from slightly different values for the reference density.

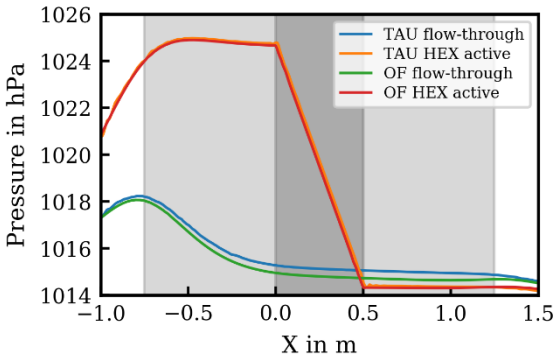

a) Static pressure

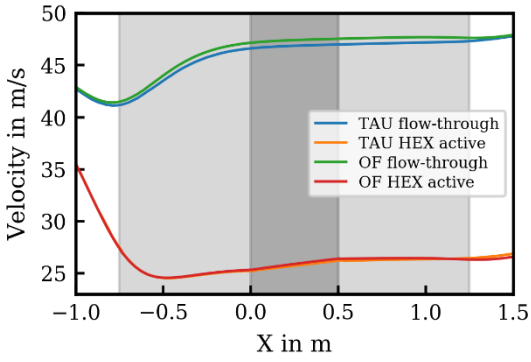

b) Velocity

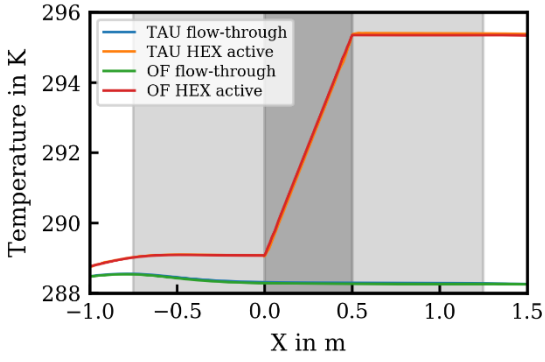

c) Static temperature

FIG 5. Comparison between the TAU and OpenFoam results.

A more detailed analysis of the results extracted at the inflow and outflow planes of the heat exchanger is provided in TAB 4. The values shown are calculated by a spatial averaging of the variables on the heat exchanger inflow and outflow planes.

Variable	HEX Setup		Value HEX Inflow Plane	Value HEX Outflow Plane	Delta (Outflow – Inflow)
Pressure	10 hPa	100 kW	1025.0/1024.4 hPa	1015.0/1014.4 hPa	-10.0/-10.0 hPa
	10 hPa	0 kW	1025.0/1024.4 hPa	1015.0/1014.4 hPa	-10.0/-10 hPa
	0 hPa	100 kW	1015.0/1015.4 hPa	1015.0/1014.7 hPa	0.0/0.7 hPa
	0 hPa	0 kW	1015.0/1014.7 hPa	1015.0/1014.7 hPa	0.0/0.0 hPa
Temperature	10 hPa	100 kW	289.0/289.0 K	295.4/296.2 K	6.4/7.2 K
	10 hPa	0 kW	289.1/289.1 K	289.1/289.1 K	0.0/0.0 K
	0 hPa	100 kW	288.3/288.5 K	291.8/292 K	3.5/3.5 K
	0 hPa	0 kW	288.3/288.3 K	288.3/288.4 K	0.0/0.1 K
Density	10 hPa	100 kW	1.23/1.23 kg/m³	1.20/1.19 kg/m³	-0.03/-0.04 kg/m³
	10 hPa	0 kW	1.23/1.23 kg/m³	1.22/1.22 kg/m³	-0.01/-0.01 kg/m³
	0 hPa	100 kW	1.23/1.23 kg/m³	1.21/1.21 kg/m³	-0.02/-0.02 kg/m³
	0 hPa	0 kW	1.23/1.22 kg/m³	1.23/1.22 kg/m³	0.0/0.0 kg/m³
Velocity	10 hPa	100 kW	25.13/25.52 m/s	25.87/26.34 m/s	0.74/0.82 m/s
	10 hPa	0 kW	25.64/25.70 m/s	25.82/26.06 m/s	0.19/0.35 m/s
	0 hPa	100 kW	45.83/46.43 m/s	46.39/47.06 m/s	0.57/0.63m/s
	0 hPa	0 kW	46.37/46.9 m/s	46.37/47 m/s	0.0/0.1 m/s
Mass flow rate	10 hPa	100 kW	15.6/15.7 kg/s	15.6/15.7 kg/s	0.0/0.0 kg/s
	10 hPa	0 kW	15.9/15.9 kg/s	15.9/15.9 kg/s	0.0/0.0 kg/s
	0 hPa	100 kW	28.2/28.5 kg/s	28.2/28.5 kg/s	0.0/0.0 kg/s
	0 hPa	0 kW	28.6/28.8 kg/s	28.6/28.8 kg/s	0.0/0.0 kg/s

TAB 4. Results for the four verification simulations with different HEX setups (TAU/OpenFoam).

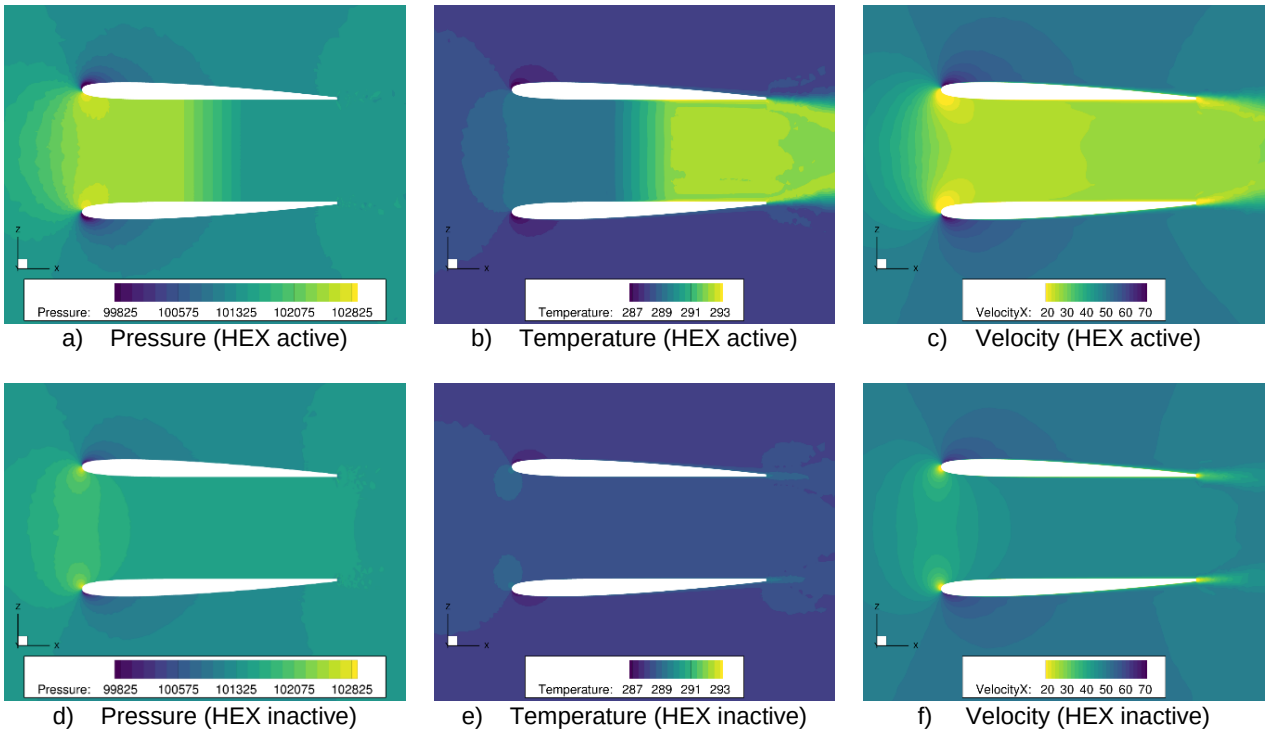

a) Pressure (HEX active) b) Temperature (HEX active) c) Velocity (HEX active)

d) Pressure (HEX inactive) e) Temperature (HEX inactive) f) Velocity (HEX inactive)

FIG 6. Symmetry plane contours for the generic nacelle with the heat exchanger model activated and de-activated.

Although OpenFOAM can account for high complexity heat transfer systems with multi-physics effects – problems that are not yet within the scope of the current TAU implementations of BFHEX – the TAU results obtained for this simplified geometry are consistent with the OpenFOAM result. Our results demonstrate that the addition of an additional heat transfer treatment into the Flowsimulator framework has resulted in a stable calculation method

which is useful for aerodynamic load calculations on aircraft with cooling systems. The pressure drop of the heat exchanger has reduced the mass flow rate through the duct by almost 50% compared to the through-flow nacelle. However, this is a function of the heat exchanger flow characteristics and highlights the need to couple calculations of this form during the initial design phase of a cooling installation.

FIG 6 shows symmetry plane contours for the static pressure, temperature and velocity for the case with BFHEX fully active and the through-flow nacelle. It can be seen that the momentum and energy induced with the body force method is evenly distributed in radial direction.

4.2. Influence of the Grid Resolution

As described in section 2, three different grid refinement levels were generated to assess the impact of the grid resolution on the modelling of the heat exchanger.

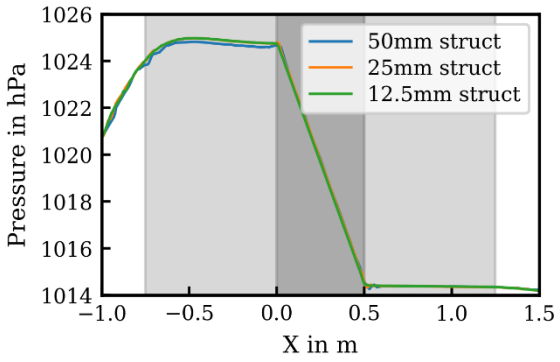

a) Static pressure

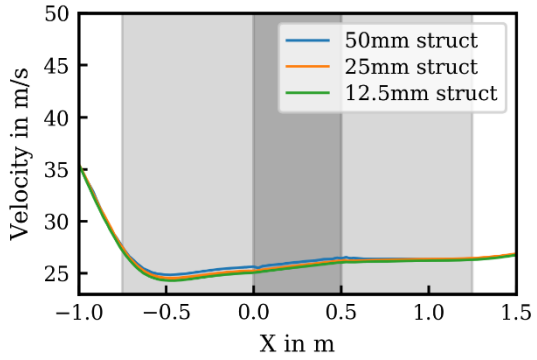

b) Velocity

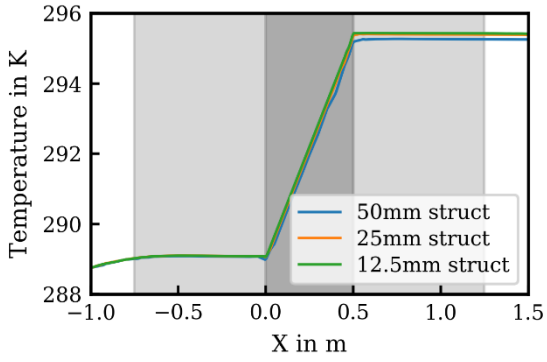

c) Static temperature

FIG 7. Velocity and temperature along the centerline of the nacelle for different cell edge length in the cooler.

FIG 7 shows the resulting curves for the velocity and temperature in the centerline of the cooler. Only the grids where a structured block was used to mesh the HEX volume are shown here. It can be seen that the temperature increase is not fully captured by the coarse grid compared to the medium and fine grid. Also, the velocity within the cooler duct changes by about 1m/s from the coarse grid to the fine grid. Although the source terms are constant in the HEX it is recommended to set the cell size within the cooler duct to at least 40 cells per HEX length to achieve a good resolution of the flow through the cooler.

4.3. Influence of the Grid Cell Type

For all refinement levels, grids with and without the structured block for the resolution of the HEX volume were generated. For these grids, the inflow and outflow plane were fully aligned to the HEX due to a modular grid generation approach.

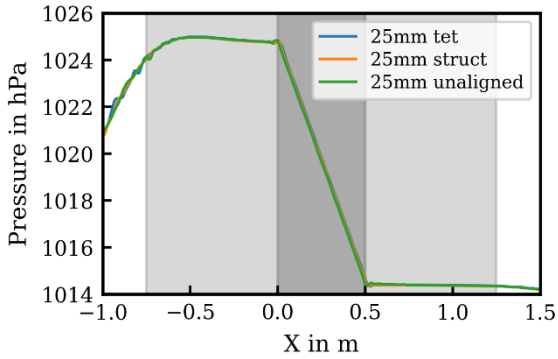

a) Static pressure

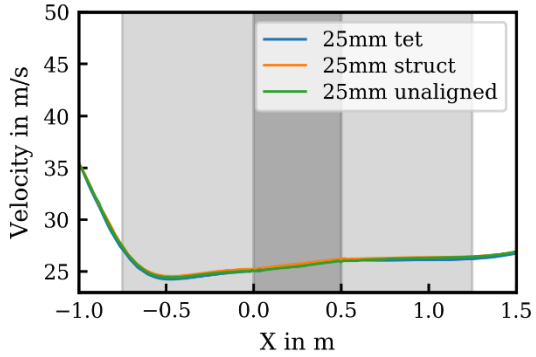

b) Velocity

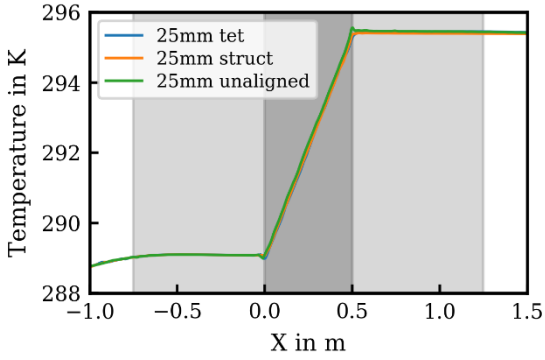

c) Static temperature

FIG 8. Pressure, velocity, and temperature along the nacelle centerline for different grid setups in the cooler.

FIG 8 shows a comparison of the results for the grids with a structured block and without a structured block (tet). In addition to these grids a grid without the modular grid generation approach was generated. This would be the most basic grid generation method and results in grid lines that are not aligned to the HEX inflow and outflow planes. The impact of the grid cell type on the velocity and temperature is small compared to the impact of the grid resolution. However, when extracting data along the centerline for the unaligned grid, small oscillations can be observed in the temperature curve at the beginning and end of the body force volume. Thus, it is recommended to use a modular grid generation approach so that the grid cells are completely aligned to the HEX inflow and outflow plane. This procedure is also suggested for the OpenFoam meshing.

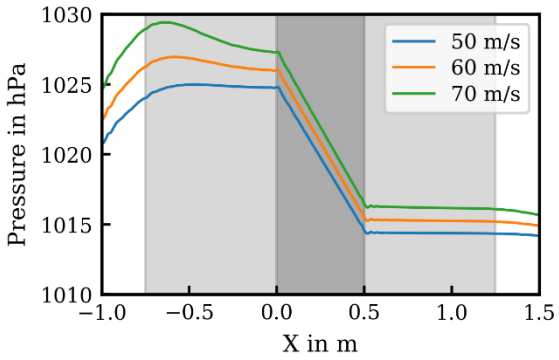

a) Static pressure

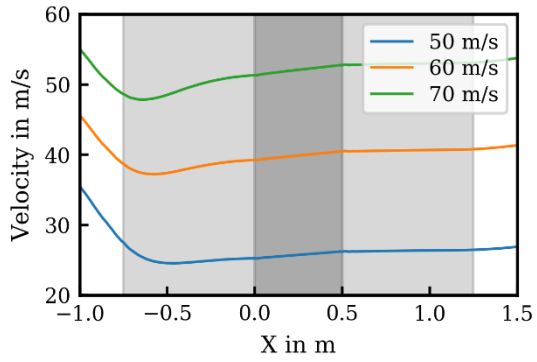

b) Velocity

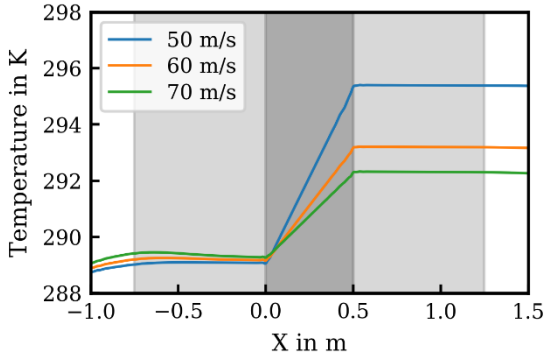

c) Static temperature

FIG 9. Pressure, velocity, and temperature along the nacelle centerline for different reference velocities.

4.4. Influence of the Reference Velocity

A variation of the velocity for the simulations was performed on the medium sized grid with a structured block for the HEX resolution in order to assess the robustness of the HEX implementation for different reference velocities and different resulting mass flow rates through the cooler. In addition to the reference velocity of 50m/s for which results have been presented in the previous sections, simulations with 30m/s, 40m/s, 60m/s, and 70m/s were conducted. The simulations with velocities lower than 50m/s are not shown here because they result in an unphysical reverse flow in the cooler due to the low flow velocity in combination with the relatively high pressure drop of the cooler. Similar results were observed for a study where the diameter of the inlet was reduced which also reduced the possible mass flow rate through the cooler.

FIG 9 shows the results for the variation of the reference velocity. The pressure drop is resolved well for all reference velocities. As expected, the velocity within the duct does not scale linearly with the reference velocity due to the impact of the pressure drop which is larger at lower flow velocities (50m/s) compared to higher flow velocities (70m/s).

The temperature development through the cooler is also as expected. The largest temperature gradient can be observed for the lowest reference velocities. The temperature rise correlates well with the analytic assumptions from equation (2) for all velocities.

As a result, it is very important for later applications to specify a pressure drop that is realistic for a certain inlet geometry and reference velocity in order to achieve an accurate modeling of the heat exchanger. If the reference velocity is too low for a certain pressure drop, the simulation of the heat exchanger can lead to unphysical results with reverse flow.

4.5. Influence of the Angle of Attack

Another very important aspect in the application of the BFHEX method for complex aircraft geometries with a cooler is the robustness of the method for different aircraft or nacelle incidence angles. Thus, a variation of the angle of attack has been performed. The symmetry plane velocity contours in the cooler are shown in FIG 10 for α=0° and α=10°. The cooler duct naturally ensures an alignment of the flow in x-direction, but the flow at the heat exchanger inflow plane is no longer uniform. Comparing the pressure drop or the temperature increase in the heat exchanger in TAB 5 shows only a small influence of the non-uniform flow through the nacelle on the temperature gradient.

	0° AoA	**10° AoA**
Pressure drop Δp	10.0 hPa	10.0 hPa
Temperature increase ΔT	6.5 K	6.4 K

TAB 5. Impact of the angle of attack on the pressure drop and temperature increase within the HEX.

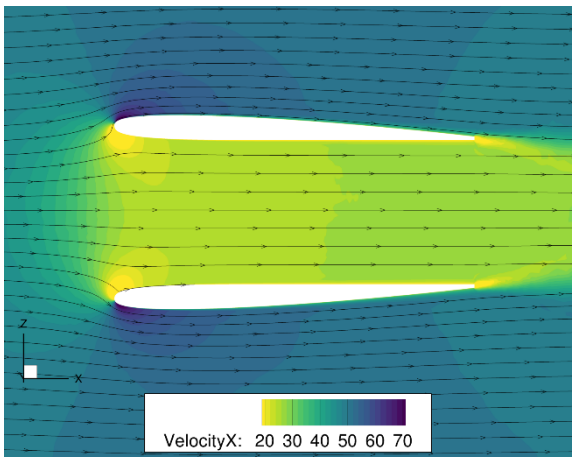

a) $\alpha = 0°$

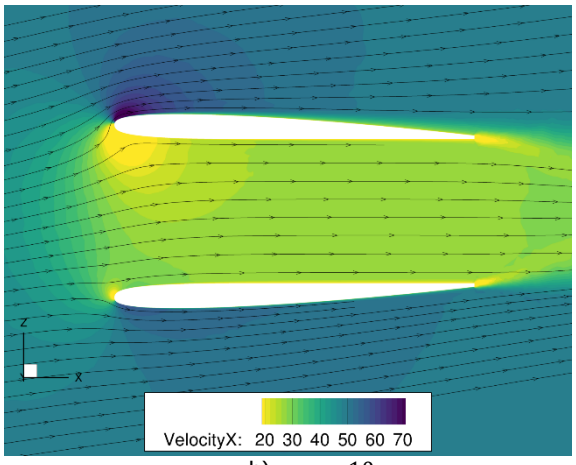

b) $\alpha = 10$

FIG 10. Symmetry plane velocity contours with and without an angle of attack.

5. INTERFACE FOR 1D HEAT EXCHANGER MODEL

The different approaches to define the pressure drop and heat flux for the BFHEX simulations were introduced in section 2. The most advanced method is a coupling of the CFD solver to a lookup table based on a 1D model of the heat exchanger. Using this lookup table, the pressure drop and heat flux of the heat exchanger can be interpolated for a certain flow condition specified by the pressure, temperature, and velocity of the flow at the HEX inflow plane. This means that during the simulation these variables have to be iteratively calculated and averaged at the inflow plane.

The easiest way to implement this was to add an additional filter to the grid that ends at the HEX inflow plane and extends exactly one grid cell upstream. For the filtered cells the average of the pressure, temperature, and velocity is calculated and used as an input for the 1D model lookup table. The filtered grid cells for the calculation of the HEX inflow parameters are highlighted in FIG 11 for different grid cell sizes in the cooler duct. The higher grid refinement will lead to smaller cells and also a smaller inlet volume reducing the error.

An iterative approach was implemented to couple the model to the CFD simulation and update the BFHEX settings while the simulation is running. For this approach, the simulation is first started without the heat exchanger activated. After initial convergence of the simulation is achieved, the iterative BFHEX model is activated. In a first step, the flow parameters at the HEX inflow plane and the resulting BFHEX settings are calculated as described previously. Subsequently the CFD solver performs a simulation with fixed body force source terms for a user defined number of inner solver iterations. These two steps are repeated until a convergence of the BFHEX settings and the flow simulation in general is achieved

6. APPLICATION FOR THE SIMULATION OF A COMPLETE AIRCRAFT

In order to verify the application of the BFHEX method for complex aircraft geometries with integrated coolers, the method was applied to two different test cases.
The first test case is a pressure recovery cooler mounted below the fuselage. A visualization is shown in FIG 12. Similar to an engine simulation, the heat exchanger is integrated into a nacelle. The challenge here is to design the diffusor and the nozzle in such a way that no separation occurs and the heat exchanger flow is optimal in terms of low losses and high cooling efficiency. In addition, this RamAir concept must be integrated on the existing fuselage (in a retro-fit design) with a minimum of drag. The results have shown that the current BFHEX implementation is robust for this test case. FIG 13 shows the second test case which represents a more complex application where the cooler is integrated in the propeller slipstream behind an actuator disk, which is not shown in the visualization. This cooler integration is advantageous because the mass flow rate through the cooler is less impacted by the low reference velocity at take-off conditions when the cooling requirements are high. However, this case shows the limitations of the developed BFHEX method. Flow separations can occur within the cooler duct due to the propeller swirl and the s-shape of the cooler duct. These flow separations lead to unphysically high temperatures in the heat exchanger.

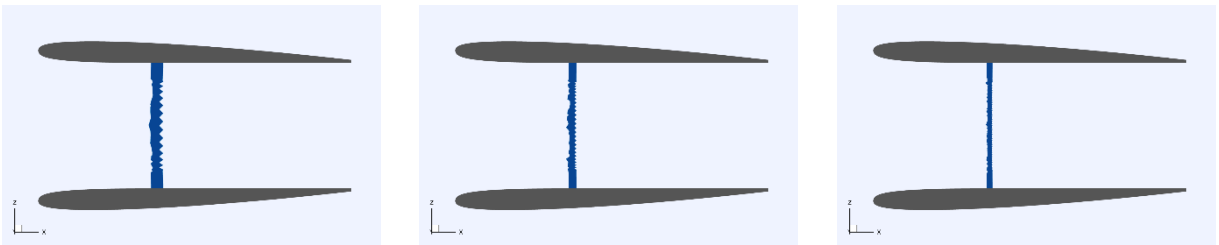

a) Coarse grid b) Medium grid c) Fine grid

FIG 11. Filtered volume for the calculation of the HEX inflow parameters.

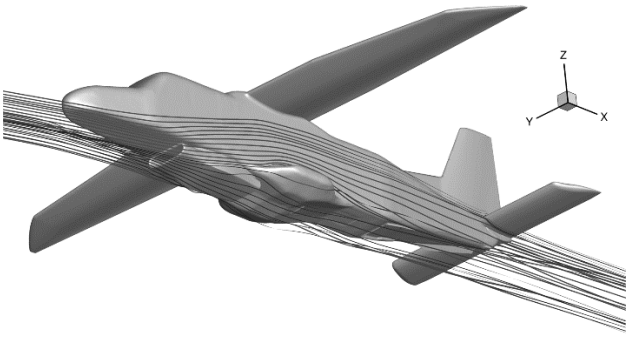

FIG 12. Heat exchanger within a RamAir concept; integrated below the fuselage of the Dornier Do 228.

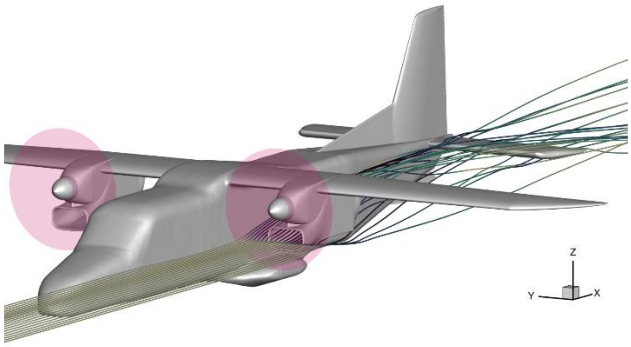

FIG 13. Visualization of a heat exchanger concept integrated in the propeller slipstream of the Dornier Do 228.

7. SUMMARY AND OUTLOOK

Recently, research on hybrid electric propulsion concepts for aircraft has increased due to the great potential to reduce the overall emissions of aviation. Fuel cells produce waste heat which has to be dissipated in heat exchangers. A novel BFHEX approach for the numerical simulation of heat exchangers was presented in this paper. It was implemented in the DLR TAU Code by utilizing the body force method in the Flowsimulator framework. A test case with an isolated axisymmetric nacelle was analyzed which showed that the approach is robust and properly resolves the underlying physics. The results of the CFD simulations were compared to analytical solutions for the pressure drop and temperature rise in the heat exchanger. The comparison between the analytic solution and the BFHEX model is very good. The impact of different grid refinement levels and grid setups has been analyzed. Fine grid resolutions with 40 cells per length of the heat exchanger are necessary to resolve the flow through the cooler properly. It was shown that a modular grid generation approach should be used so that the grid cells are aligned to the HEX inflow and outflow plane.

First applications for the new method were presented for a fuselage-mounted cooler as well as for a nacelle-mounted cooler. The BFHEX implementation is ready for the design of the pressure recovery cooler and will now be applied to optimize both the drag impact due to the integration of the cooler as well as the heat exchanger performance.

The test case with a nacelle mounted heat exchanger showed the limitations of the current state of the BFHEX implementation. One main challenge for the next version of BFHEX is to properly resolve the physics of a heat exchanger with small areas of separated flow in the cooler duct. In order to achieve this, a geometrical blockage term and a non-uniform distribution of the body force source terms will be implemented.

In the future, the BFHEX method will be applied in the design of hybrid electric aircraft with a focus on the aerodynamic interactions and high-fidelity simulation of integration effects of heat exchangers in complex aircraft geometries.

8. ACKNOWLEGEMENTS

The authors gratefully acknowledge the valuable discussions with MTU about the numerical simulation of heat exchangers.

9. REFERENCES

[1] D. S. Lee, D. W. Fahey, M. R. Skowron, M. R. Allen and U. Burkhardt, "The contribution of global aviation to anthropogenic climate forcing for 2000 to 2018," *Atmospheric Environment,* vol. 244, p. 117834, 2021.

[2] DLR, BDLI, "Zero Emission Aviation - German Aviation Research White Paper," 2020.

[3] McKinsey & Company, "Hydrogen-powered aviation - A fact-based study of hydrogen technology,," 2020.

[4] EG&G Technical Services, Inc., "Fuel Cell Handbook," U.S. Department of Energy, 2004.

[5] B. Eisfeld and M. Ruetten, "A Coupled Heat Exchanger Boundary Condition for Pre-Design of Air-Intake Positions," in *50th AIAA Aerospace Sciences Meeting*, Nashville, TN, 2012.

[6] A. Raichle, S. Melber-Wilkending und J. Himisch, „A new Actuator Disk Model for the TAU Code and application to a sailplane with a folding engine," STAB-Symposium, 2006.

[7] S. Spinner, M. Trost and R. Schnell, "An Overview of High Fidelity CFD Engine Modeling," in *AIAA SciTech*, San Diego, 2022.

[8] H. Weller, G. Tabor, H. Jasak und Fureby, Christer, „A Tensorial Approach to Computational Continuum Mechanics Using Object Orientated Techniques," *Computers in Physics,* Bd. 12, pp. 620-631, 1998.

[9] D. A. Nield und A. Bejan, Convection in Porous Media, Springer, 2013.

[10] W. Thollet, „Body Force Modeling of Fan-Airframe Interactions," Ph.D. Thesis, Toulouse, 2017.

[11] D. Schwamborn, T. Gerhold und R. Heinrich, „The DLR TAU-Code: Recent Applications in Research and Industry," in *ECCOMAS CFD 2006 CONFERENCE*, Delft, 2006.

[12] P. R. Spalart und S. R. Allmaras, „A One-Equation Turbulence Model for Aerodynamic Flows," in *30th Aerospace Sciences Meeting and Exhibit*, Reno, NV, 1992.